

# Accelerated K-Serial Stable Coalition for Dynamic Capture and Resource Defense

Junfeng Chen, Zili Tang and Meng Guo

**Abstract**—Coalition is an important mean of multi-robot systems to collaborate on common tasks. An effective and adaptive coalition strategy is essential for the online performance in dynamic and unknown environments. In this work, the problem of territory defense by large-scale heterogeneous robotic teams is considered. The tasks include surveillance, capture of dynamic targets, and perimeter defense over valuable resources. Since each robot can choose among many tasks, it remains a challenging problem to coordinate jointly these robots such that the overall utility is maximized. This work proposes a generic coalition strategy called K-serial stable coalition algorithm (KS-COAL). Different from centralized approaches, it is distributed and anytime, meaning that only local communication is required and a K-serial Nash-stable solution is ensured. Furthermore, to accelerate adaptation to dynamic targets and resource distribution that are only perceived online, a heterogeneous graph attention network (HGAN)-based heuristic is learned to select more appropriate parameters and promising initial solutions during local optimization. Compared with manual heuristics or end-to-end predictors, it is shown to both improve online adaptability and retain the quality guarantee. The proposed methods are validated rigorously via large-scale simulations with hundreds of robots, against several strong baselines including GreedyNE and FastMaxSum.

## I. INTRODUCTION

Multi-robot systems can be extremely efficient when solving a team-wide task in a concurrent manner. The key to efficiency is an effective strategy for collaboration to improve overall utility, where different robots form coalitions to tackle a common task, e.g., multiple UAVs surveil an area for intruders by dividing it into respective regions [1], [2]; multiple UGVs capture an intruder by approaching from different directions [3], [4]. However, when there are a large amount of diverse tasks to be accomplished, the optimal collaboration strategy is significantly more difficult to derive, as each robot needs to choose among numerous potential coalitions, yielding a combinatorial explosion in complexity [5], [6]. Such difficulty is further amplified when the set of tasks is generated online non-deterministically and attached to dynamic objects, e.g., intruders enter the area from unknown positions and move constantly within. In these scenarios, an adaptive collaboration strategy is essential to dynamically adjust coalitions online and re-assign robots to new tasks [7]. Furthermore, when the numbers of robots and tasks are large, a centralized coordinator that assigns coalitions centrally quickly becomes inadequate, especially for the dynamic scenario. Instead, a decentralized

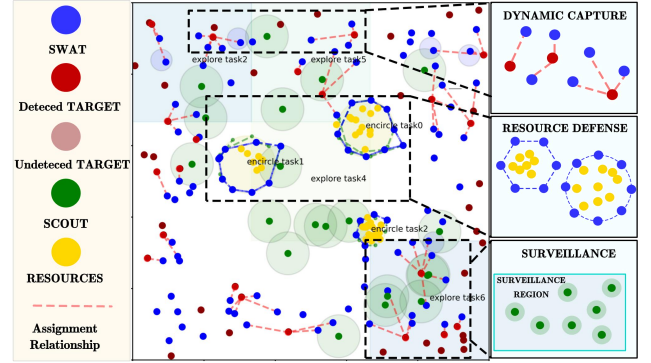


Fig. 1. Snapshots of the simulated scenario: 100 UGVs as swat robots and 20 UAVs as scout robots coordinate distributedly and simultaneously three different tasks including surveillance of over 50 unknown target robots and 100 unknown resources, dynamic capture of detected targets, and defense over detected resources.

coalition strategy is more suitable [8], [9], where each robot coordinates with other robots via local communication.

### A. Related Work

This work focuses on the particular application of deploying fleets of UAVs and UGVs for three different tasks: the surveillance over a territory, the capture of potential intruders, and the defense of valuable resources. Many recent work tackles each of these tasks, e.g., the collaborative exploration or coverage problem [1], [2]; the well-known pursuit-evasion problem [3], [4], [10]; the perimeter defense problem [11]. Various extensions can be found where the team size, capability, environment model changes. For instances, an optimal pursuit strategy is designed in [12] first for the 2v2 perimeter defense problem, and then extended to  $NvM$  cases in a greedy way. The work in [13] employs a graph-theoretic approach to ensure the distance-based observation graph remains connected, i.e., the evaders are always visible. A flexible strategy is proposed in the recent work [14], which can enclose and herd evaders to designated areas. The work in [15] proposes an encirclement strategy for the slow pursuers to capture the faster evader. However, these tasks are often considered *separately* and *individually* in the aforementioned work. Thus, the proposed methods therein can not be applied directly when the same team of heterogeneous robots are responsible for a dynamic combination of these three tasks.

On the other hand, the task assignment for multi-agent systems refers to the process of assigning a set of tasks to the agents, see [16], [17] for comprehensive surveys. Well-known problems include the classic one-to-one assignment

The authors are with the College of Engineering, Peking University, Beijing 100871, China. This work is supported by the Natural Science Foundation of China (NSFC) under grant 62203017; and by the Ministry of Education under grant 2021ZYA05004; Contact: meng.guo@pku.edu.cn.

problem [18], the multi-vehicle routing problem [17], and the coalition structure generation (CSG) problem [19]. Representative methods include the Hungarian method [18], the mixed integer linear programming (ILP) [16] and the search-based methods [20]. However, these methods typically rely on the static table of agent-task pairwise cost. Such cost matrix *does not exist* for any of three tasks considered here. More specifically, the benefit of one robot joining a coalition depends mainly on other robots that are already in the coalition, which often decreases drastically as more robots join the same coalition. Consequently, these existing methods for task assignment are not suitable for this application.

Lastly, the CSG problem mentioned above is the most relevant as it is particularly suitable for collaborative tasks, see the comprehensive study in [6]. A market-based coalition formation algorithm is presented in [21], with no clear guarantee on the solution quality. Provably optimal algorithms are proposed in [5], which has not been applied to large-scale systems due to combinatorial complexity. Thus, distributed and anytime approaches are proposed in [8], [9], which are designed to solve static coalition formation problems. Notably, learning-based methods are proposed in [22], [23] to learn via reinforcement learning or supervised learning to mimic an expert solver. However, the learned heuristic in this work is used to *accelerate* the model-based algorithm, instead of replacing it as a black-box predictor.

### B. Our Method

To overcome these limitations, this work proposes a distributed coalition strategy for heterogeneous robots under the tasks of dynamic capture and resource defense. Its backbone is the K-serial stable coalition algorithm (KS-COAL), which is a distributed, anytime and complete algorithm designed for generic definition of collaborative tasks. It is particularly suitable for large-scale robotic teams under unknown and dynamic environments, where the tasks are generated and changed online. Model-based motion strategies and utility functions are designed for each type of tasks (i.e., exploration, capture and defense), which are adaptive to team sizes and environment features. It is proven formally to be anytime, complete and strictly better than the popular Nash-1-stable solutions. To further improve the solution quality within a limited computation time, the KS-COAL algorithm is accelerated by a heuristic estimation of the relative importance among the robots given the current task distribution. This heuristic is learned offline based on optimal solutions of small-scale problems and heterogeneous graph attention networks (HGAN) as the network structure. Consequently, the learned policy is integrated seamlessly with the KS-COAL algorithm. The proposed method is validated extensively on large-scale simulations against several strong baselines, and extended to different applications to show its generalization.

Main contributions of this paper are summarized as follows: (i) an unified framework for distributed task coordination of multi-agent systems under diverse tasks; (ii) a coordination algorithm with provable guarantee of quality; (iii) a supervised learning mechanism to accelerate the online coordination process, without losing the quality guarantee.

## II. PROBLEM DESCRIPTION

### A. Workspace and Robot Description

Consider a group of robots  $\mathcal{R}$  that co-exist in a common workspace  $\mathcal{W} \subset \mathbb{R}^2$ . Each robot  $i \in \mathcal{R}$  is described by three components: (i) Motion model. Each robot follows the unicycle model with state  $s_i$  as the 2D coordinates and orientation, and input  $u_i$  as the angular and linear velocities; (ii) Perception model. Each robot can observe fully the environment within its sensing radius  $r_i > 0$ ; (iii) Action model. There are three teams of robots with distinctive capabilities: (i) SCOUT team  $\mathcal{R}_o \subset \mathcal{R}$  that moves swiftly and is capable of long-range perception; (ii) SWAT team  $\mathcal{R}_c \subset \mathcal{R}$  that is capable of short-range perception but specialized for capturing other robots that are less than  $d_c > 0$  in distance; and (iii) TARGET team  $\mathcal{R}_s \subset \mathcal{R}$  that is capable of mid-range perception and can take “resources” within the workspace that are less than  $d_s > 0$  in distance. In other words, the scout robots, typically UAVs, can navigate easily around the workspace to locate any target robot and resources, such that the swat robots, typically UGVs, can approach and capture the target robots or form encirclement to defend resources.

Lastly, it is assumed that robots within the scout and swat team can communicate freely without any range limitation, the same applies to robots within the target team. However, they can not eavesdrop over other teams communication.

### B. Resource Generation

To mimic the realistic scenario of perimeter defense with valuable resources, it is assumed that one resource  $\xi_t$  is generated every period  $T_r > 0$  around several clusters within the workspace. Formally, it is generated following a Gaussian Mixture Model (GMM) e.g.,

$$\xi_t \sim \text{GMM}(\{(\alpha_k, \mu_k, \Sigma_k)\}), \quad (1)$$

where  $(\alpha_k, \mu_k, \Sigma_k)$  are the weight, mean and covariance of Gaussian component  $G_k$ . The distribution of these clusters is static but *unknown* initially, thus can only be estimated online. After generation, one resource remains available until it is taken by a target robot. New resources are constantly generated by the distribution above. Denoted by  $\Xi_t$  the set of resources that are available at time  $t \geq 0$ , which is set to  $\emptyset$  initially.

Meanwhile, each target robot  $i \in \mathcal{R}_s$  searches for resources within its sensing range via random exploration. Once one resource is found, the robot approaches it via the shortest path and takes it if still available, while avoiding being captured by the swat team. If a target robot is captured, it is immobilized and can not take resources anymore.

### C. Problem Formulation

The overall objective is to design a *distributed* control strategy for the scout and swat teams, such that the number of captured target robots subtracting the number of resources taken by the target team is maximized.

**Remark 1.** The desired strategy is distributed, meaning that there exist no central coordinator that assigns globally the next control and action for each robot. Instead, the scout and swat

robots synthesize the best strategy for the team collaboratively, via local communication and coordination. ■

### III. PROPOSED SOLUTION

The proposed solution is a distributed framework for task coordination and motion control. It consists of three main building blocks: (i) the motion strategies for the scout and swat team are introduced in Sec. III-A; (ii) given the proposed utility function, the distributed coordination algorithm KS-COAL is described in Sec. III-B which is proven to be anytime and complete; (iii) to facilitate faster adaptation to dynamic changes during online execution, a HGAN-based accelerator for the distributed algorithm is designed in Sec. III-C.

#### A. Task Definition and Motion Strategy

This section describes three different types of tasks and the associated motion strategies as illustrated as shown in Fig. 2: particularly, the online detection of target robots and resources by the scout robots; the dynamic capture of target robots by the swat robots; and the encirclement of resources by the swat robots. Additionally, a utility function is defined for possible coalitions w.r.t. each task, which serves as a fundamental component for the coalition formation algorithm later.

1) *Collaborative Exploration and Detection*: Without loss of generality, the workspace is divided into a set of regions, denoted by  $\mathcal{W} = \{r_m\}$ . It can be feature-based such as regions of interest or geometry-based such as triangular [24] or uniform grids. Each region contains one exploration task for the team of scout robots. The potential gain of visiting region  $r_m$  is given by:

$$\chi(r_m) = u_c(r_m) + \rho_{tg}(r_m) + \rho_{rs}(r_m), \quad (2)$$

where  $u_c(r_m) = 1 - \lambda^{-t_e}$  measures the uncertainty regarding the properties of region  $r_m$ , with  $t_e$  being the last time region  $r_m$  was visited by a scout robot,  $\lambda \in (0, 1)$  being a design parameter;  $\rho_{tg}(r_m), \rho_{rs}(r_m)$  measure the density of targets and resources within each region. If  $\chi(r_m)$  is detected to be higher than a predefined threshold, a exploration task  $\omega_m$  is broadcaster among the scout robots.

The exploration strategy by several scout robots is relatively simple: the region is divided equally by the number of agents and each agent swipes one sub-region. The exploration task is finished once all robots within the coalition finish exploring their respective areas. Given the above strategy, the associated utility function  $f_{exp}$  is given by:

$$f_{exp}(\hat{\mathcal{R}}_o, \omega_m) \triangleq \frac{\chi(r_m)}{\tau(\hat{\mathcal{R}}_o, r_m)}, \quad (3)$$

where  $\hat{\mathcal{R}}_o \subset \mathcal{R}_o$  is the subset of scout robots potentially assigned to the exploration task  $\omega_m$ ;  $\chi(r_m)$  is defined in (2); and  $\tau(\hat{\mathcal{R}}_o, r_m)$  estimates the task duration by:

$$\tau(\hat{\mathcal{R}}_o, r_m) \triangleq \max_{i \in \hat{\mathcal{R}}_o} \left\{ t_i(s_i, r_m) + \frac{A_m}{2\hat{N}_s R_i v_i} \right\}, \quad (4)$$

where  $t_i(s_i, r_m)$  measures the time needed for agent  $i \in \hat{\mathcal{R}}_o$  to travel to region  $r_m$  from its position  $s_i$ ;  $A_m$  is the total

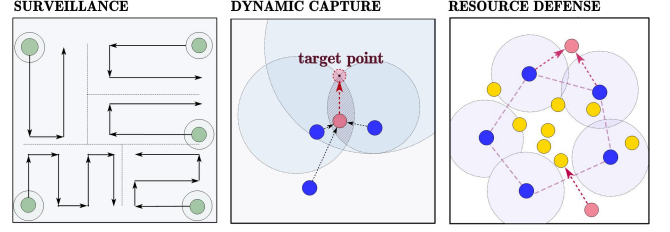


Fig. 2. Illustration of the motion strategies for three different tasks.

area of region  $r_m$ ;  $\hat{N}_s = |\hat{\mathcal{R}}_o|$ ;  $2R_i v_i$  is the area explored by agent  $i$  per unit time with  $R_i, v_i$  being its detection radius and reference velocity. Thus, the total duration is determined by the slowest robot. In other words, the marginal utility is low if a robot joins a large coalition from a far distance.

2) *Collaborative Capture*: Once target robots are detected by the scout robots via exploration, their positions are broadcasted to all swat robots. Consequently, each target robot is associated with a capture task. A collaborative capture strategy similar to [25] is followed for multiple swat robots.

More specifically, consider a subset of swat robots  $\hat{\mathcal{R}}_c \subseteq \mathcal{R}_c$  that forms a coalition to capture one target robot  $j \in \mathcal{R}_s$ . Each robot  $i \in \hat{\mathcal{R}}_c$  follows the pure pursuit strategy by constantly adjusting its orientation to head towards the target robot and moving with a constant velocity  $v_i$ . On the other hand, the target robot tries to survive the longest time by heading towards the farthest point in  $\hat{\mathcal{C}}_j \triangleq \bigcap_i \mathcal{C}_{ij}$ , as the intersection area of all Apollonius circles  $\mathcal{C}_{ij}$  of swat robot  $i \in \hat{\mathcal{R}}_c$  and the target robot  $j$ ; the Apollonius circle  $\mathcal{C}_{ij}$  is defined as:

$$\mathcal{C}_{ij} = \left\{ s \in \mathbb{R}^2 \mid \|s - s_i\| \leq \frac{v_i}{v_j} \|s - s_j\| \right\}, \quad (5)$$

where  $(s_i, v_i), (s_j, v_j)$  are the position and reference velocity of robots  $i, j$ . It has been shown in [25] that via the above motion strategy, the target robot would be captured with  $\hat{\mathcal{C}}_j$  eventually. The capture task is finished once the target robot is captured and becomes immobile.

Accordingly, the utility of depolying coalition  $\hat{\mathcal{R}}_c$  for the capture task  $\omega_j$  of robot  $j$  is given by:

$$f_{cap}(\hat{\mathcal{R}}_c, \omega_j) \triangleq \Gamma - \min_{i \in \hat{\mathcal{R}}_c} \left\{ t_i(\hat{\mathcal{C}}_j, s_i) \right\}, \quad (6)$$

where  $\Gamma > 0$  is a design parameter to balance different tasks;  $t_i(\hat{\mathcal{C}}_j, s_i)$  estimates the least time needed for robot  $i$  to reach the capture region  $\hat{\mathcal{C}}_j$  from its position  $s_i$ .

3) *Resource Defense via Encirclement*: Given the detected resources by scout robots, the underlying Gaussian clusters  $\{G_k\}$  in (1) can be identified by maximum-likelihood estimation [26]. Afterwards, to further defend these resources from being taken by target robots, swat robots can form circles around these clusters via the *encirclement* strategy, similar to [14]. In particular, consider a subset of swat robots  $\hat{\mathcal{R}}_c \subseteq \mathcal{R}_c$  and one cluster  $G_k$  of which the encirclement task is denoted by  $\omega_k$ . First, a circle centered at  $\mu_k$  with radius  $3\sigma_k$  is computed as the defense perimeter. Then, the swat robots in  $\hat{\mathcal{R}}_c$  navigate to this circle and keep an even distance with each other, to defend an equal segment of the circle. Afterwards, the swat robots remain static and capture

any target robot that enters its capture radius. The encirclement task is accomplished after a given period and the agents are released. Via the above motion strategy, the following utility function is proposed:

$$f_{\text{enc}}(\hat{\mathcal{R}}_c, \omega_k) \triangleq \text{sat} \left( \sum_{i \in \hat{\mathcal{R}}_c} \frac{d_{c,i}}{3\pi\sigma_k} \right), \quad (7)$$

where  $\hat{\mathcal{R}}_c \subseteq \mathcal{R}_c$  contains the swat robots within the coalition;  $d_{c,i}$  is the capture radius of robot  $i$ ;  $3\pi\sigma_k$  is the radius of the formed circle; thus  $d_{c,i}/(3\pi\sigma_k)$  estimates the portion of circle defended by the robot  $i \in \hat{\mathcal{R}}_c$ ;  $\text{sat}(\cdot)$  is a clip function for output interval  $[0, 1]$ . Thus, the maximum number of swat robots within the encirclement is reached when the summation of their portions is closest to but less than one. Afterwards, the total utility remains unchanged if more swat robots join as their capture regions largely overlap.

### B. Distributed Coalition Formation

Given the above three types of tasks and the associated utility function described in Sec. III-A, the next prominent step is to form coalitions within the team of swat and scout robots such that the overall utility for the team is optimized. Different from most relevant work that focuses on a centralized solution for static scenes, this work proposes a *unified, anytime* and *distributed* algorithm that can handle a large number of exploration, capture and defense tasks in dynamic and time-varying environments.

1) *Problem Reformulation*: To begin with, the task assignment problem is formulated based on the coalition formation literature [6], [7]. Particularly, consider the following definition of a coalition structure:

$$\mathcal{F} \triangleq (\mathcal{R}, \Omega, f, \mathcal{K}), \quad (8)$$

where  $\mathcal{R} = \{1, \dots, N\}$  is the team of  $N$  robots;  $\Omega = \{\omega_1, \dots, \omega_M\}$  is the set of  $M$  tasks;  $f : 2^{\mathcal{R}} \times \Omega \rightarrow \mathbb{R}^+$  is the utility function of a potential coalition for any given task in  $\Omega$ ;  $\mathcal{K} = \{k_1, \dots, k_N\}$  is the optimality index for each robot, which is assumed to be static for now but adaptive in the overall algorithm presented in the sequel. The set of tasks that can be performed by robot  $i$  is denoted by  $\Omega_i$ .

**Definition 1** (Assignment). A valid solution of the coalition structure  $\mathcal{F}$  in (8) is called an assignment, denoted by  $\nu = \{(\omega_m, \mathcal{R}_m), \forall \omega_m \in \Omega\}$ , where  $\mathcal{R}_m \subset \mathcal{R}$  represents a coalition that performs the common task  $\omega_m \in \Omega$ , and  $\mathcal{R}_{m_1} \cap \mathcal{R}_{m_2} = \emptyset, \forall m_1 \neq m_2$ . Moreover, an assignment is called optimal if its mean utility, i.e.,

$$\varrho(\nu) \triangleq \frac{\sum_{\omega_m \in \Omega} f(\mathcal{R}_m, \omega_m)}{M}, \quad (9)$$

is maximized, and denoted by  $\nu^*$ . ■

Note that the mean utility above is chosen to be consistent with the main objective. With a slight abuse of notation, let  $\nu(\omega_m) = \mathcal{R}_m$  which returns the coalition for task  $\omega_m$  and conversely,  $\nu(i) = \omega_m$  which returns the task assigned to robot  $i, \forall i \in \mathcal{R}_m$ . More importantly, an assignment  $\nu$  can be modified via the following switch operation by any robot.

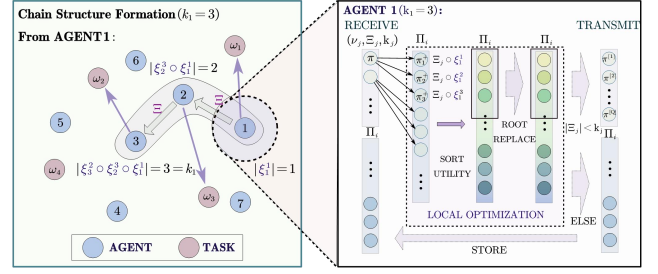


Fig. 3. Illustration of key steps in the KS-COAL algorithm: distributed exchange via the chain structure (left) and local optimization (right).

**Definition 2** (Switch Operation). The operation that robot  $i \in \mathcal{R}$  is assigned to task  $\omega_m \in \Omega$  is called a *switch* operation, denoted by  $\xi_i^m$ . The switch  $\xi_i^m$  is valid only if  $\omega_m \in \Omega_i$ . Thus, via  $\xi_i^m$ , an assignment  $\nu$  is changed into a new assignment  $\hat{\nu}$ , such that  $\hat{\nu}(i) = \omega_m$ . For brevity, denote by  $\hat{\nu} = \xi_i^m(\nu)$ . ■

**Definition 3** (Chain Transformation). A *transformation* is defined as a chain of allowed switches, i.e.,

$$\Xi \triangleq \xi_{i_1}^{m_1} \circ \xi_{i_2}^{m_2} \circ \xi_{i_\ell}^{m_\ell} \dots \circ \xi_{i_L}^{m_L}, \quad (10)$$

where  $L$  is the total length;  $i_{\ell+1} \in \mathcal{N}_\ell$  is the constraint of forming a chain,  $\forall \ell = 0, \dots, L-1$ . The transformation  $\Xi$  is valid if all switches inside are valid. Thus, via  $\Xi$ , an assignment  $\nu$  can be transformed into a new assignment  $\hat{\nu}$ , by recursively applying the switches  $\xi_{i_\ell}^{m_\ell} \in \Xi$ , such that  $\hat{\nu}(i_\ell) = \omega_{m_\ell}, \forall \ell = 0, \dots, L-1$ . For brevity, denote by  $\hat{\nu} = \Xi(\nu)$ . ■

**Definition 4** (Rooted Transformation). A rooted transformation at robot  $i \in \mathcal{R}$  is denoted by  $\Xi_i$ , which is a chain transformation that starts from  $i$ , i.e.,  $i_1 = i$  in (10). ■

**Remark 2.** The chain transformation above is different from “arbitrary modification” in [7], where the sequence of transformations can be operated on any robot. However, the chain structure in (10) requires that only neighboring robots can perform switches consecutively. The main motivation is to limit the search space of possible transformations to robots within the  $K$ -hop local communication network, thus accelerating the convergence to a high-quality solution. ■

**Definition 5** ( $\mathcal{K}$ -Serial Stable). An assignment  $\nu^*$  is  $\mathcal{K}$ -Serial stable (KSS), if for each robot  $i \in \mathcal{R}$ , there does not exist *any* rooted transformation  $\Xi_i$  such that: (i)  $\Xi_i$  is valid; (ii)  $\varrho(\Xi_i(\nu^*)) > \varrho(\nu^*)$ ; (iii)  $|\Xi_i| \leq k_i$ , where  $k_i$  is the optimality index defined in (8). ■

**Remark 3.** The above notion of KSS solution contains the Nash equilibrium in [7] and the globally optimal solution as special cases. Namely, if the indices are chosen that  $k_i = 1, \forall i \in \mathcal{R}$ , then the KSS solution is equivalent to the Nash equilibrium as at most one robot is allowed to switch its own task. If  $k_i = N, \forall i \in \mathcal{R}$  and the communication graph is connected, then the KSS solution is equivalent to the globally optimal solution as all robots can switch tasks simultaneously. Thus, the parameter  $\mathcal{K} = \{k_i\}$  provides the flexibility to adaptively improve the solution given the time budget. ■

**Problem 1.** Given the coalition structure  $\mathcal{F}$  in (8), design a distributed algorithm to find one KSS solution by Def. 5. ■

2) *Algorithm Description:* A fully-distributed, asynchronous and anytime algorithm called the  $\mathcal{K}$ -serial stable coalition (KS-COAL) is proposed to solve Problem 1. As shown in Fig. 3, the main idea is to combine distributed inter-robot message passing and local optimization. Each robot  $i$  attempts to find the locally-best transformation rooted at itself, which can improve the currently-known best solution the most. In addition, each robot also participates in the optimization of transformations rooted at other robots, i.e., as part of the chain defined in (10). Lastly, a consensus protocol is continuously running in parallel to encourage the convergence to a common KSS solution across the team.

More specifically, as summarized in Alg. 1, each robot follows the same algorithmic procedure asynchronously. Initially at  $t = 0$ , each robot computes the set of initial partial solutions by assigning one executable task to itself. Then, robot  $i$  sends the message below to all its neighbors  $j \in \mathcal{N}_i$ :

$$\pi_{i \rightarrow j} \in \{(\nu_0, \varepsilon, k_i), \nu_0(i) = \omega_m \in \Omega_i\}, \quad (11)$$

where  $\nu_0$  is the partial initial solution,  $\varepsilon$  denotes the null transformation and  $k_i$  is the optimality index of robot  $i$ . Additionally, this message is added to a local message buffer denoted by  $\Pi_i$ , see Line 1.

At  $t > 0$ , each robot  $i \in \mathcal{N}$  follows the same round of sending messages, receiving messages, local optimization and consensus as in Lines 3-15. To begin with, for any stored message, when  $\pi = (\nu, \Xi, k) \in \Pi_i$   $|\Xi| \leq k_i$  namely  $|\Xi| \leq k$  holds, robot  $i$  relays this message to its neighbors, i.e.,  $\pi_{i \rightarrow j} = \pi$ ,  $\forall j \in \mathcal{N}_i$ . Meanwhile, after receiving each message  $\pi_{j \rightarrow i}$  from robot  $j$  that  $i \in \mathcal{N}_j$ , it stores  $\pi_{j \rightarrow i}$  in its buffer  $\Pi_i$ . During local optimization, robot  $i$  generates a new message  $\pi^+$  for any selected message  $\pi = (\nu, \Xi, k) \in \Pi_i$  by appending an additional switch operation to the existing transformation, i.e.,

$$\pi^+ = (\nu, \Xi \circ \xi_i^m, k), \quad (12)$$

where  $\nu$  is the same initial solution as in  $\pi$ ;  $\xi_i^m$  assigns task  $\omega_m$  to robot  $i$ . Note that this modification is only allowed if  $|\Xi| \leq k$ , i.e., its length limit is not reached. This new message  $\pi^+$  is stored in  $\Pi_i$  and thus later shared with its neighbors, see Line 9-10. More importantly, robot  $i$  maintains the best assignment that is currently-known to itself, denoted by  $\nu_i^*$ . It is updated each time a message is received or a new message is generated in (12), i.e.,

$$\nu_i^* = \Xi(\nu), \quad \text{if } \rho(\Xi(\nu)) > \rho(\nu_i^*), \quad (13)$$

as in Line 11, where the updated utility  $\rho(\Xi(\nu))$  can be computed locally by robot  $i$  as  $\rho(\Xi(\nu)) = \rho(\nu_i^*) + \nabla_f(\omega_m) + \nabla_f(\omega'_m)$ , where  $\omega_m, \omega'_m$  are tasks assigned to robot  $i$  before and after the update, respectively; and  $\nabla_f(\cdot)$  is the difference in task utility of  $\omega_m, \omega'_m$  before and after the update.

As mentioned earlier, a consensus protocol is executed in parallel, such that the team converges to the same KSS solution. However, this should be done in special care to avoid pre-mature termination and over-constrained search space. In particular, each robot  $i$  shares its best solution  $\nu_i^*$  in (12) with its neighbors, i.e., by sending directly the associated message  $\pi_i^*$ , then robot  $i$  can locally compute the best assignments received from other robots, namely,  $\rho(\nu_j^*)$  as in Line 12.

---

**Algorithm 1:** KS-COAL algorithm.

---

**Input:** Coalition structure  $\mathcal{F}$ .

**Output:** KSS solution  $\nu^*$ .

```

/* Message passing */
1 Initialize  $\Pi_i$  by (11),  $\Pi_i^* = \emptyset$ ;
2 while not terminated do
    /* Sending message */
3   for  $\pi = (\nu, \Xi, k) \in \Pi_i$  and  $|\Xi| \leq k$  do
4     Send  $\pi_{i \rightarrow j}$  to  $\mathcal{N}_i$ ;
5     Remove  $\pi_{i \rightarrow j}$  from  $\Pi_i$ ;
    /* Receiving message */
6   forall  $i \in \mathcal{R}$  do
7     Receive  $\{\pi_{j \rightarrow i}\}$  and update  $\Pi_i$ ;
    /* Local optimization */
8   for  $\pi = (\nu, \Xi, k) \in \Pi_i$  do
9     Compute  $\xi_i^m$  and  $\pi^+$  by (12);
10    Save  $\pi^+$  to  $\Pi_i$ ;
11    Update  $\nu_i^*$  by (13);
    /* Consensus */
12   if  $\rho(\nu_j^*) > \rho(\nu_i^*)$  then
13      $\nu_i^* \leftarrow \nu_j^*$ ;
14     Compute  $\{\Xi_i(\nu_i^*)\}$  and update  $\Pi_i$  by (14);
15     Update  $\nu_i^*$  by (13);

```

---

Afterwards, robot  $i$  updates its best assignment if any received assignment yields a better overall utility, i.e.,  $\rho(\nu_j^*) > \rho(\nu_i^*)$ . Then, all rooted transformations  $\{\Xi_i\}$  stored in  $\Pi_i$  should be applied to  $\nu_i^*$  to generate new solutions  $\{\Xi_i(\nu_i^*)\}$ , i.e.,

$$(\nu, \Xi_i, k_i) \rightarrow (\nu_i^*, \Xi_i, k_i), \quad (14)$$

as in Line 14. Meanwhile, these invalid messages are removed from  $\Pi_i$ . Thus, the new assignment is given by  $\Xi_i(\nu_i^*)$ , of which the utility is computed by tracing back the chain operations in  $\Xi_i = \xi_{i_1}^{m_1} \circ \xi_{i_2}^{m_2} \cdots \circ \xi_{i_L}^{m_L}$  and querying each robot  $i_\ell$  along the chain directly the change of utility. If any of these new assignments in  $\{\Xi_i(\nu_i^*)\}$  yields a better utility than  $\nu_i^*$ , it replaces  $\nu_i^*$  and is shared with the neighbors, see in Line 15. If the local best assignment  $\nu_i^*$  remains unchanged after a certain number of rounds, the algorithm terminates.

3) *Performance Analysis:* Under the proposed algorithm, convergence to a KSS solution is ensured by the theorem below. Furthermore, it is shown that this solution extends naturally to the globally optimal solution if  $\mathcal{K}$  is set accordingly.

**Theorem 1.** Under Alg. 1, the local assignment is ensured to converge to  $\nu_i^* = \nu^*$ ,  $\forall i \in \mathcal{R}$ , where  $\nu^*$  is a KSS solution.

*Proof.* For each robot  $i$ , all rooted transformations  $\{\Xi_i\}$  with  $|\Xi_i| \leq k_i$  are generated eventually via the proposed communication protocol within its  $k_i$ -hop communication network. Namely, the solution  $\nu^*$  is contained within this set. Furthermore, due to the updating mechanism of  $\nu_i^*$ , if  $\nu_i^*$  remains unchanged for all robots  $i \in \mathcal{R}$ , it means  $\nu_i^*$  can not be improved by any rooted transformation  $\{\Xi_i\}$  with  $|\Xi_i| \leq k_i$ . If  $\nu_i^* = \nu^*$ ,  $\forall i \in \mathcal{R}$ , then  $\nu^*$  is a KSS solution by Def. 5.  $\square$

**Corollary 1.** Given that  $k_i = N$ ,  $\forall i \in \mathcal{R}$ , the KSS solution return by Alg. 1 is the globally optimal solution.



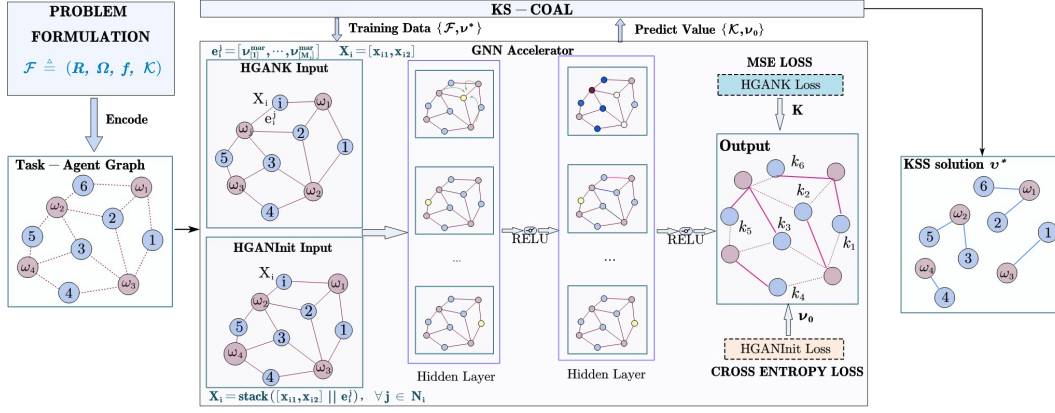


Fig. 4. Network structure of the proposed NAC: the HGAN-K branch (**upper**) and the HGAN-Init branch (**lower**) that predicts the parameter  $\mathcal{K}$  and initial solution  $\nu_0$ , which are used to accelerate the KS-COAL algorithm.

*Proof.* Assume that  $\nu^* \neq \nu^\dagger$ , where  $\nu^\dagger$  is the optimal assignment. Since the communication graph is connected, there must exist a chain transformation  $\Xi$  of length  $N$  to generate  $\nu^\dagger$ . Since  $\nu^*$  is KSS, meaning that  $\varrho(\nu^\dagger) \leq \varrho(\nu^*)$ , it results in a contradiction. Thus,  $\nu^* = \nu^\dagger$  holds.  $\square$

### C. Neural Accelerator for Dynamic Adaptation

Since all robots are *constantly* moving and resources are generated dynamically, the current assignment might not be optimal or even feasible at latter time. Moreover, simply re-triggering the same Alg. 1 all the time might be computationally prohibitive or causes oscillations due to inconsistent assignments. Additionally, in many cases only a few robots need to adjust their assignments. Thus, a neural accelerator (NAC) based on heterogeneous graph attention networks (HGAN) from [27] is proposed to accelerate the proposed KS-COAL. Specifically, it predicts directly the choice of parameter  $\mathcal{K}$  and an initial solution for KS-COAL, by taking as inputs the distribution of all robots and tasks.

1) *Network Structure of NAC:* As shown in Fig. 4, the proposed HGAN model contains two branches called HGAN-K and HGAN-Init, which are used to predict the  $\mathcal{K}$  and  $\nu_0$ , respectively. They both share the common two HGAN middle-layers to extract the hidden embedding. As inputs to both branches, two labelled graphs are constructed based on the same underlying coalition structure. In particular, three types of robots and three types of tasks are encoded as vertices with different attributes. Undirected edges from robots to tasks indicate whether one robot can participate in one task. Both node and edge attributes are encoded *differently* within HGAN-K and HGAN-Init: (i) The attribute of each edge in HGAN-K is a vector of marginal utility given by:

$$v(i, \omega_m) = \left\{ f(\mathcal{R}_m, \omega_m) - f(\mathcal{R}_m \setminus \{i\}, \omega_m), \forall \mathcal{R}_m \in \hat{\mathcal{R}}_m \right\},$$

where  $i \in \mathcal{R}_m$  is any coalition that can perform task  $\omega_m \in \Omega$ ;  $\hat{\mathcal{R}}_m \subset 2^{\mathcal{R}}$  is the set of all such coalitions;  $v \in \mathbb{R}_{\geq 0}^{|\hat{\mathcal{R}}_m|}$  is a vector of non-negative reals. However, the edges for HGAN-Init are attribute-free and are only responsible for passing messages. (ii) Each vertex in HGAN-K is labelled by their robot or task type. However, each vertex in HGAN-Init is encoded by stacking  $v(i, \omega_m)$  above for all possible tasks.

Zero-padding is applied to ensure that these attributes have consistent sizes across vertices and edges. These graphs are then processed by the HGANs tailored for heterogeneous graphs with varying sizes. As results, HGAN-K outputs the predicted parameter  $\mathcal{K}$  over each robot vertex, while HGAN-Init outputs a ranking over all edges of each robot vertex.

2) *Training and Execution:* To begin with, the training data is collected by solving the considered scenario by the proposed KS-COAL, under different random seeds. More specifically, it is given by  $\mathcal{D} = \{(\mathcal{F}, \mathcal{K}, \nu^*)\}$ , where the tuple consists of a problem instance  $\mathcal{F}$  in (8) under a random choice of  $\mathcal{K}$  within  $\{1, 2, 3\}$ ;  $\mathcal{K}$  is the optimal choice for each robot, and the associated KSS assignments  $\nu^*$  obtained by KS-COAL. First, each problem instance is transformed into labelled graphs as described above, while the optimal robot-task pairs are derived from  $\nu^*$  and the optimal choice of  $\mathcal{K}$  is quantized into  $\{1, 2, 3\}$  given  $J^*$ , where  $J^* \in \mathbb{Z}^N$  is the total number of switches that each robot  $i \in \mathcal{N}$  has performed and resulted in an increase of the overall utility. Then, the HGAN-K and HGAN-Init branches are both trained in a supervised way, where “Weighted MSE loss” is chosen as the loss function for HGAN-K to avoid imbalanced data, and “Cross Entropy loss” for HGAN-Init. Note that during training the modern HGANs recursively update the edge features by aggregating information within multiple-hop neighborhoods. Consequently, the trained HGAN-K can predict the optimal choice of  $\mathcal{K}$ , while the HGAN-Init outputs directly a recommended solution  $\nu_0$ .

During execution, each robot constructs its local multi-hop graphs given a new problem  $\mathcal{F}$ , which is encoded in the same way as the training process. Then, this labelled local graph is fed into the learned HGAN to obtain the hidden embedding, which is then aggregated via local communication with neighboring robots. Consequently, after convergence, the aggregated embedding is used to predicate the optimal choice of  $k_i$  and  $\omega_m$  for each robot  $i \in \mathcal{N}$ . Thus, the KS-COAL algorithm can be kick-started with this choice of  $\mathcal{K}$  and this initial assignment  $\nu_0$ . It is worth mentioning that the guarantee on solution quality in Theorem 1 is still retained.

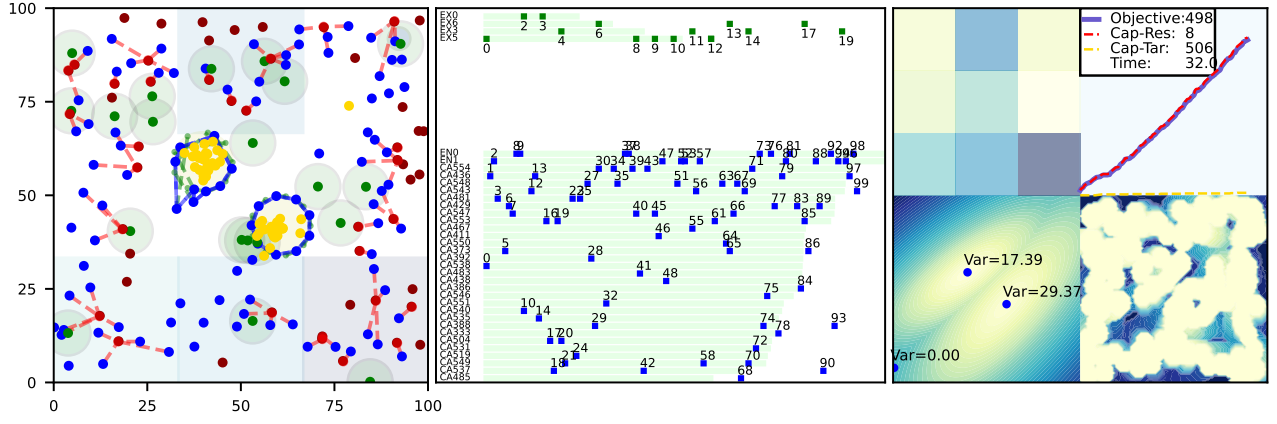


Fig. 5. One snapshot of the task execution: motion of all robots (**left**), results of dynamic task assignment (**middle**), estimated distribution of resources and targets (**bottom-right**), number of captured targets and preserved resources (**top-right**).

#### D. Computation Complexity

Since Alg. 1 is fully distributed, its complexity is analyzed for a single robot. For one round of communication, robot  $i$  can send at most  $|\Pi_i|$  messages to  $|\mathcal{N}_i|$  robots. Thus, the worst time-complexity for sending messages is  $\mathcal{O}(N_{\Pi}N_r)$ , where  $N_{\Pi}$  is the upperbound of  $|\Pi_i|$  and  $N_r < N$  is the upperbound of  $|\mathcal{N}_i|$ . Similarly, the stage of “local optimization” has the time-complexity  $\mathcal{O}(N_{\Pi}N_{\omega})$ , where  $N_{\omega}$  is the maximum number of the tasks that one robot is capable. Thus, the overall time-complexity at each iteration is  $\mathcal{O}(N_{\Pi}(2N_r + N_{\omega}))$ . Note that  $N_{\Pi}$  is upper bounded by  $(N_{\omega}N_r)^{k_{\max}}$ , where  $k_{\max} = \max_i \{k_i\}$ . Furthermore, since the exact time of convergence  $\bar{t}$  is hard to determine, a factor  $\epsilon$  is introduced to relax the convergence criterion. More specifically, it can be regarded as “convergence” if there is no  $\Xi$  that can improve the utility  $\rho$  by more than  $\epsilon$ . For a single robot, the number of effective switches is upper bounded by:  $\Delta\rho/\epsilon$ , where  $\Delta\rho$  is the upper bound of  $\rho^* - \rho$ . Since the iterations required for “consensus” is bounded by  $N$  between two effective switches, it holds that  $\bar{t} \leq \frac{\Delta\rho}{\epsilon}N$ . Thus, the overall time-complexity of Alg. 1 is given by  $\mathcal{O}((N_{\omega}N_r)^{k_{\max}}(2N_r + N_{\omega})(\Delta\rho/\epsilon)N)$ .

### IV. NUMERICAL EXPERIMENTS

Extensive simulation experiments are conducted for large-scale systems, which are compared against several strong baselines. The proposed method is implemented in Python3 with Pytorch geometric Graph (PyG) from [28] and tested on an AMD 7900X 12-Core CPU @ 4.7GHz with RTX-3070 GPU. More detailed descriptions and experiment videos can be found in the supplementary file.

#### A. Setup

1) *Agent and Workspace Model*: As shown in Fig. 5, consider 100 swat robots, 20 scout robots, and 50 target robots in a free workspace of size  $100m \times 100m$ . Their reference velocities are set to  $1m/s$ ,  $6m/s$  and  $0.9m/s$ . The sensing radius is set to  $5m$  for swat robots and  $10m$  for scout robots. The capture range of swat and target robots are set to  $3m$  and  $2m$ . Moreover, the resources are generated by three Gaussian clusters of variance  $0.75m$  every  $5s$ . Note that the initial distribution of target robots and resources are unknown to the

swat and scout robots. Captured targets and taken resources are removed from display. In addition, the workspace is divided into 9 regions for the surveillance task. The rest of system model follows the descriptions in Sec. III-A.

2) *Proposed Method and Baselines*: Parameters for the proposed utility functions are set to  $t_e = 40s$  in (2) and  $\Gamma = 200$  in (6). Both HGAN-K and HAGAN-Init in the proposed NAC have 2 SAGEConv layers and 128 hidden channels, with the aggregation scheme of “mean”. There are in total **7 baselines** compared with the proposed NAC: (i) the KS-COAL algorithm with the parameter  $\mathcal{K}$  uniformly set to 2 or 3 or randomly, denoted by **KS2**, **KS3** and **Random**, respectively; (ii) two variants of the NAC for ablation study: **NACK** that only uses the learned accelerator to predict  $\mathcal{K}$  with the initial solution being the previous solution, and **NACInit** that only predicts the initial solution with a random  $\mathcal{K}$ ; (iii) two state-of-the-art methods for distributed coordination: **GreedyNE** from [9], where a Nash-stable assignment is selected; **FastMaxSum** from [29], which solves the matching problem over a task-robot biparte graph via distributed message passing.

#### B. Results

As illustrated in Fig. 5, the robot motion and actions are monitored during execution, with a display of the dynamic task assignment. In addition, distribution of the detected target robots and resources are also estimated along with the number of captured targets and preserved resources. The proposed NAC is triggered every 5 time step, during which 20 rounds of communication is allowed. Thus, it follows that (i) the scout robots are assigned to different partitions according to actual distribution of target robots and resources. It can be seen that three clusters of resources are gradually identified. (ii) once the swat robots receive the position of target robots from the scout robots, they follow the distributed coordination process to capture target robots and form encirclement around cluster of resources. It is interesting to notice that some swat robots remain static when the marginal utility of joining a capture or defense task is negligible. Also, some swat robots may switch from a defense task to a capture task when some target robots are close-by and require a collaborative capture. In total, 50 resources are preserved and 234 target robots are captured over 200 time steps.

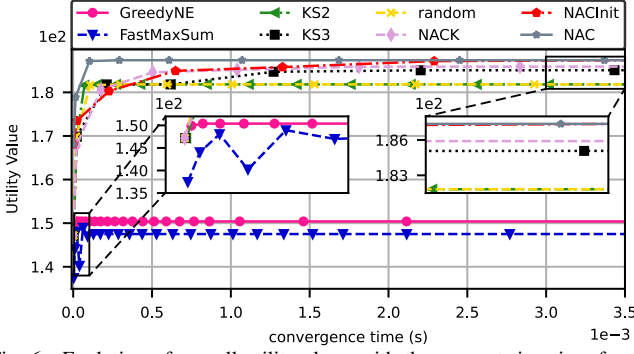


Fig. 6. Evolution of overall utility along with the computation time for our method NAC and 7 other baselines.

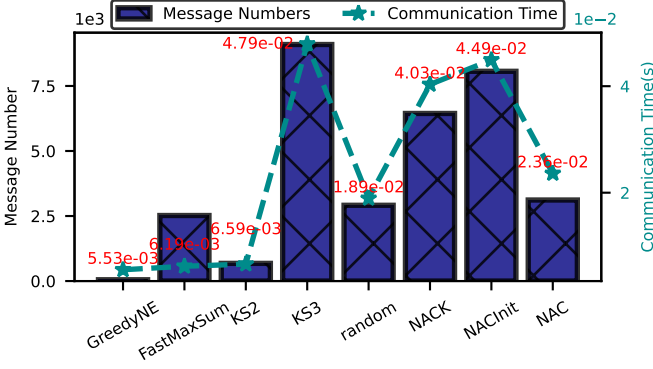


Fig. 7. The number of messages and communication time of all methods.

### C. Comparisons

1) *Convergence over a Fixed Problem*: To begin with, the baselines are compared to solve the *same* coalition problem, formulated based on one snapshot of dynamic scene above. All baselines are given the same amount of computation iterations and communication iterations. Evolution of the total utility along with the iterations is shown in Fig. 6. Our method **NAC** has a faster convergence than **KS2** and **KS3** (0.5ms vs. 1.0ms and 3.0ms), but with the highest utility after convergence (187.4 vs 181.8 and 185.1). It confirms our analyses that larger  $\mathcal{K}$  requires longer sequence of transformation and thus slower to converge. The proposed **NAC** predicts  $\{k_i\}$  among  $\{1, 2, 3\}$  and accelerate the convergence even further by predicting also an initial solution, compared with even **KS2**. On the other hand, it is interesting to note that since **KS3** can not converge at each iteration under limited computation time, it can not achieve the highest utility and less than **NAC**. Both **GreedyNE** and **FastMaxSum** reach convergence within only 0.1ms and 0.2ms, however with a final utility significantly less than than **KS3** and **NAC** ((150.4, 147.5) vs. (185.1, 187.4)). Last but not least, compared with **NAC**, **NACK** converges slower (2.0ms) and has a worse utility 185.9. It is worth noting that although trained by data from **KS3**, **NACInit** outperforms **KS3** with both a higher initial and final utility 185.1 and 187.4. This verifies that both the parameter  $\mathcal{K}$  and the initial solution  $\nu_0$  are worth learning to accelerate the coordination process.

2) *Communication Overhead*: All methods are executed for 20 iterations and the total amount of exchanged messages is compared. As shown in Fig. 7, it is clear that drastically more messages are generated as the parameter  $\mathcal{K}$  increases i.e., 50,

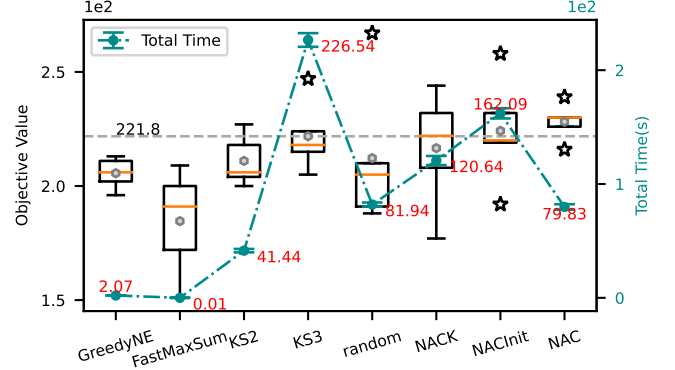


Fig. 8. Overall long-term utility and total time elapsed of all methods.

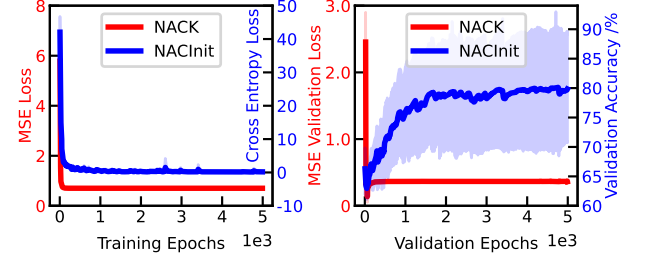


Fig. 9. Loss during training and validation for HGAN-K and HGAN-Init.

680, 9094 for **GreedyNE**, **KS2** and **KS3**, respectively. Both **NACK** and **NACInit** generate less messages than **KS3** (6443 and 8064 vs. 9094), due to either smaller  $\mathcal{K}$  or faster convergence. Notably, our **NAC** requires merely 3116 messages to reach convergence, drastically less than both variants **NACK** and **NACInit**. This signifies the effect of acceleration via the **NAC**. Lastly, **FastMaxSum** requires more messages than **KS2** but less than **KS3** however with different structure.

3) *Long-term Performance over Dynamic Scenes*: The described experiment are repeated 10 times with different random seeds for 200 time steps. As summarized in Fig. 8, our **NAC** drastically improves the accumulated performance by 11% in average compared with **GreedyNE** and 24% than **FastMaxsum**. In contrast, **KS3** without the neural accelerator achieves an accumulated utility 8% higher than **GreedyNE**. Similar to the static scenario, both **NACK** and **NACInit** have less overall performance compared with our **NAC** (216.6, 224.2 vs. 228.2). This indicates that both branches of **NAC** can facilitate faster adaptation in dynamic scenarios thus improving long-term performances.

### D. Generalization Analyses

To verify how the proposed **NAC** generalizes to different scenes and system sizes, the following two aspects are tested.

1) *Validation Accuracy*: As shown in Fig. 9, both the HGAN-K and HGAN-Init models converge after respectively 500, 2000 epochs during learning. Both models are tested in different validation sets, which are generated and shuffled by running diverse scenarios of different random seeds. It can be seen that the HGAN-K model has close to 0.2 mse loss, while the HGAN-Init model reaches 80% accuracy, which is caused by the fact that due to the limitations of computation resource and time, the diversity of train datasets is not sufficient to generalize other unseen data.



Method	Overall Utility (Case 1-4)
GreedyNE	(77, 247, 1202, 169)
FastMaxSum	(24, 189, 823, 159)
<b>NAC</b>	<b>(86, 296, 1274, 203)</b>

TABLE I  
COMPARISON WITH TWO BASELINES IN SYSTEM SIZES.

2) *Novel Scenarios*: Three different scenarios are designed with different system sizes, and different distribution of swat and target robots: (i) *Case 1*, with 40 swat robots and 20 target robots in the team; (ii) *Case 2*, with 40 swat robots and 100 target robots; (iii) *Case 3*, with 150 swat robots and 100 target robots; (iv) *Case 4*, with 150 swat robots and 20 target robots. These systems are executed under the *same* learned **NAC** and other baseline methods, of which the results are summarized in the Tab. I. It can be seen that our **NAC** outperforms **GreedyNE** and **FastMaxSum** for all three cases in terms of overall utility.

## V. CONCLUSION

A fully-distributed and generic coalition strategy called KS-COAL is proposed in this work. Different from most centralized approaches, it requires only local communication and ensures a K-serial Nash-stable solution upon termination. Furthermore, HGAN-based heuristics are learned to accelerate KS-COAL during dynamic scenes by selecting more appropriate parameters and promising initial solutions. Future work includes more complex collaborative tasks.

## REFERENCES

- [1] A. Khan, B. Rinner, and A. Cavallaro, "Cooperative robots to observe moving targets," *IEEE transactions on cybernetics*, vol. 48, no. 1, pp. 187–198, 2016.
- [2] R. S. De Moraes and E. P. De Freitas, "Multi-uav based crowd monitoring system," *IEEE Transactions on Aerospace and Electronic Systems*, vol. 56, no. 2, pp. 1332–1345, 2019.
- [3] T. H. Chung, G. A. Hollinger, and V. Isler, "Search and pursuit-evasion in mobile robotics," *Autonomous robots*, vol. 31, no. 4, pp. 299–316, 2011.
- [4] I. E. Weintraub, M. Pachter, and E. Garcia, "An introduction to pursuit-evasion differential games," in *2020 American Control Conference (ACC)*. IEEE, 2020, pp. 1049–1066.
- [5] T. Michalak, T. Rahwan, E. Elkind, M. Wooldridge, and N. R. Jennings, "A hybrid exact algorithm for complete set partitioning," *Artificial Intelligence*, vol. 230, pp. 14–50, 2016.
- [6] T. Rahwan, T. P. Michalak, M. Wooldridge, and N. R. Jennings, "Coalition structure generation: A survey," *Artificial Intelligence*, vol. 229, pp. 139–174, 2015.
- [7] Q. Li, M. Li, B. Q. Vo, and R. Kowalczyk, "An anytime algorithm for large-scale heterogeneous task allocation," in *International Conference on Engineering of Complex Computer Systems (ICECCS)*, 2020, pp. 206–215.
- [8] F. M. Delle Fave, A. Rogers, Z. Xu, S. Sukkarieh, and N. R. Jennings, "Deploying the max-sum algorithm for decentralised coordination and task allocation of unmanned aerial vehicles for live aerial imagery collection," in *IEEE International Conference on Robotics and Automation*, 2012, pp. 469–476.
- [9] F. Prántare and F. Heintz, "An anytime algorithm for optimal simultaneous coalition structure generation and assignment," *Autonomous Agents and Multi-Agent Systems*, vol. 34, no. 1, pp. 1–31, 2020.
- [10] T. Olsen, A. M. Tumlin, N. M. Stiffler, and J. M. O’Kane, "A visibility roadmap sampling approach for a multi-robot visibility-based pursuit-evasion problem," in *IEEE International Conference on Robotics and Automation (ICRA)*, 2021, pp. 7957–7964.
- [11] J. Paulos, S. W. Chen, D. Shishika, and V. Kumar, "Decentralization of multiagent policies by learning what to communicate," in *International Conference on Robotics and Automation (ICRA)*, 2019, pp. 7990–7996.
- [12] E. Garcia, D. W. Casbeer, A. Von Moll, and M. Pachter, "Multiple pursuer multiple evader differential games," *IEEE Transactions on Automatic Control*, vol. 66, no. 5, pp. 2345–2350, 2020.
- [13] V. G. Lopez, F. L. Lewis, Y. Wan, E. N. Sanchez, and L. Fan, "Solutions for multiagent pursuit-evasion games on communication graphs: Finite-time capture and asymptotic behaviors," *IEEE Transactions on Automatic Control*, vol. 65, no. 5, pp. 1911–1923, 2019.
- [14] V. S. Chipade and D. Panagou, "Multiagent planning and control for swarm herding in 2-d obstacle environments under bounded inputs," *IEEE Transactions on Robotics*, vol. 37, no. 6, pp. 1956–1972, 2021.
- [15] X. Fang, C. Wang, L. Xie, and J. Chen, "Cooperative pursuit with multi-pursuer and one faster free-moving evader," *IEEE transactions on cybernetics*, 2020.
- [16] A. Torreño, E. Onaindia, A. Komenda, and M. Štolba, "Cooperative multi-agent planning: A survey," *ACM Computing Surveys (CSUR)*, vol. 50, no. 6, pp. 1–32, 2017.
- [17] M. Gini, "Multi-robot allocation of tasks with temporal and ordering constraints," in *AAAI Conference on Artificial Intelligence*, 2017.
- [18] R. Jonker and T. Volgenant, "Improving the hungarian assignment algorithm," *Operations Research Letters*, vol. 5, no. 4, pp. 171–175, 1986.
- [19] R. Massin, C. J. Le Martret, and P. Ciblat, "A coalition formation game for distributed node clustering in mobile ad hoc networks," *IEEE Transactions on Wireless Communications*, vol. 16, no. 6, pp. 3940–3952, 2017.
- [20] R. Fukasawa, H. Longo, J. Lysgaard, M. P. De Aragão, M. Reis, E. Uchoa, and R. F. Werneck, "Robust branch-and-cut-and-price for the capacitated vehicle routing problem," *Mathematical programming*, vol. 106, no. 3, pp. 491–511, 2006.
- [21] L. Vig and J. A. Adams, "Multi-robot coalition formation," *IEEE transactions on robotics*, vol. 22, no. 4, pp. 637–649, 2006.
- [22] C. De Souza, R. Newbury, A. Cosgun, P. Castillo, B. Vidolov, and D. Kulić, "Decentralized multi-agent pursuit using deep reinforcement learning," *IEEE Robotics and Automation Letters*, vol. 6, no. 3, pp. 4552–4559, 2021.
- [23] L. Zhou, V. D. Sharma, Q. Li, A. Prorok, A. Ribeiro, P. Tokekar, and V. Kumar, "Graph neural networks for decentralized multi-robot target tracking," in *IEEE International Symposium on Safety, Security, and Rescue Robotics (SSRR)*, 2022, pp. 195–202.
- [24] C. Belta, V. Isler, and G. J. Pappas, "Discrete abstractions for robot motion planning and control in polygonal environments," *IEEE Transactions on Robotics*, vol. 21, no. 5, pp. 864–874, 2005.
- [25] A. Von Moll, D. W. Casbeer, E. Garcia, and D. Milutinović, "Pursuit-evasion of an evader by multiple pursuers," in *2018 International Conference on Unmanned Aircraft Systems (ICUAS)*, 2018, pp. 133–142.
- [26] T. Toda, A. W. Black, and K. Tokuda, "Voice conversion based on maximum-likelihood estimation of spectral parameter trajectory," *IEEE Transactions on Audio, Speech, and Language Processing*, vol. 15, no. 8, pp. 2222–2235, 2007.
- [27] X. Wang, H. Ji, C. Shi, B. Wang, Y. Ye, P. Cui, and P. S. Yu, "Heterogeneous graph attention network," in *The world wide web conference*, 2019, pp. 2022–2032.
- [28] M. Fey and J. E. Lenssen, "Fast graph representation learning with PyTorch Geometric," in *ICLR Workshop on Representation Learning on Graphs and Manifolds*, 2019.
- [29] Q. Li, "Task allocation and team formation in large-scale heterogeneous multi-agent systems," Ph.D. dissertation, Swinburne University Of Technology, 2022.